# Trinarization of μX-ray CT Images of Partially Saturated Sand at Different Water-Retention States Using a Region Growing Method

Yosuke Higo[1], Fusao Oka[2], Ryoichi Morishita[3], Yoshiki Matsushima[4] and Tatsuya Yoshida[4]

[1]Department of Urban Management, Kyoto University, Japan

[2]Professor Emeritus, Kyoto University, Japan

[3]Graduate student, Department of Civil and Earth Resources Engineering, Kyoto University, Japan

[4]Former graduate student, Department of Civil and Earth Resources Engineering, Kyoto University, Japan

**Keywords:** trinarization, microfocus X-ray CT, partially saturated sand, water-retention state, region growing method

## ABSTRACT

The trinarization of micro-computed tomography (CT) images for partially saturated soils at different water-retention states has been performed to clearly identify the three phases, i.e., the soil particles, the pore water and the pore air. We have proposed a trinarization technique for partially saturated soils whose histograms of the gray values for the three phases overlap each other. The segmentation method used in this study is the region growing method that ensures the spatial continuity of the phases extracted by the segmentation. Micro CT images of a dense sand specimen during the wetting process in a water retention test have been obtained. It has been found that the trinarization of the CT images in a high pore saturation regime provides reasonable results, while that in a low pore saturation regime overestimates the local void ratio. This is because the gray values of the mixels of the soil particle phase and the air phase, due to the partial volume effect, are similar to those of the water phase. It is necessary, therefore, to validate the trinarization results, by a comparison with the test results, because it is difficult to theoretically evaluate the partial volume effect. The correction of the tolerance value for the low pore saturation case with validation has provided better trinarization results. Through the trinarized CT images, the form of the existing pore water at different water-retention states has been discussed.

## 1. INTRODUCTION

Partially saturated soils are composed of soil particles, pore water and pore air. It is well known that the pore water between the soil particles of partially saturated soils exists in the form of menisci for which the pore water pressure is negative when the air pressure is zero. The negative pressure, namely, suction, provides an increase in the inter-particle force, which in turn causes an increase in the strength and the deformation characteristics of the partially saturated soils. On the other hand, an increase in the water content brings about a loss in suction due to the infiltration of water and/or shearing, which causes the degradation of the strength and stiffness and often leads to the brittle behaviour of partially saturated soils, such as the collapse of embankments. Hence, to understand the mechanical behaviour of partially saturated soils, it is important to know the relation between the suction and the water content, i.e., the water-retention curve, which is also closely related to the seepage behaviour in partially saturated soils. From a macroscopic point of view, the water-retention curves during both the wetting process and the drying process have been widely understood through water-retention tests on soils specimens. Up to now, however, the microscopic water-retention behaviour of partially saturated soils has been conceptually explained by schematic figures (e.g., Bear 1979, Kohgo et al. 1993). This is simply because it has been difficult to observe the microscopic water-retention behaviour.

In the last decade, micro-computed tomography (CT) techniques have been developed to view the inside of objects with a microns' level of high spatial resolution. Microfocus X-ray CT, referred to as μX-ray CT hereinafter, is one of the most powerful tools for viewing the microstructures of partially saturated sand, such as particulate structures, void spaces and pore water. Recently, the microstructures of partially saturated soils have been visualized using μX-ray CT by the authors' group and other researchers (e.g., Higo et al. 2011, Yoshida et al. 2011, Riedel et al. 2012, Higo et al. 2013).

The identification of the soil particles, the pore water and the pore air, provided by the trinarization of the CT images, is helpful for studying the microstructures of partially saturated soils. For the following reasons, however, the trinarization of CT images is usually not straightforward: (1) The inherent wide variety of gray values for the CT images, using a broad spectrum of X-rays generated by a bremsstrahlung source, leads to the overlapping of the three phases in the histograms. (2) The 'mixels' caused by the partial volume effect of the two phases are possibly similar to the other phase.

The aim of the present study is to propose a reasonable trinarization technique for the CT

images of three-phase mixed partially saturated soils. In this study, μX-ray CT scanning for a partially saturated sand specimen during the wetting process of a water-retention test has been conducted. In addition, a trinarization technique with a region growing method has been proposed. The region growing method is one of the region-based segmentation methods for digital images (e.g., Rozenfeld and Kak 1982; Adams and Bischof 1994). The trinarization method has been adopted for the μX-ray CT images to distinguish the soil particles, the pore water and the pore air from each other. In particular, trinarizations in both high and low pore saturation regimes have been carried out. Through a comparison of the two cases, trinarization at different water retention states has been discussed.

## 2. WATER RETENTION TEST WITH X-RAY CT SCANNING

### 2.1 μX-ray CT system

The μX-ray CT system used in this study is KYOTO-GEOμXCT (TOSCANER-32250μHDK). The focus size of the microfocus X-ray tube is small, 4μm, which provides the highest spatial resolution of 5μm. The system also has a relatively high X-ray energy due to the maximum voltage of 225 kV and the maximum current of 1mA. The magnification factor can be arbitrarily selected, since the focus-center distance (FCD) and the focus-image distance (FID) can both be manually adjusted. The specifications include the image matrix size of 1024×1024 in the case of the cone-beam scan. For more details, see Higo et al. (2011). Since a bremsstrahlung source is used, the X-rays have a broad spectrum. The CT images in the present study have 16-bit gray values. In the CT images shown in this paper, the gray values have been linearly transformed into 8-bit monochrome data.

### 2.2 Testing material and preparation of specimen

The test sample used in this study is Toyoura silica sand, whose physical properties include an average diameter of 0.185 mm, a particle density of 2.64 g/cm$^3$, a maximum void ratio of 0.975 and a minimum void ratio of 0.614. Toyoura sand is classified as a semi-angular uniform sand with a uniformity coefficient of 1.6.

The specimen was prepared by the water sedimentation technique to make it almost water-saturated. Air-dried sand was poured into the stainless split mould whose inner walls were covered with a membrane and filled up with distilled water. The specimen was compacted by tapping the outside of the mould. The void ratio was 0.706, corresponding to a relative density of 74.5%, the height was 41.4 mm and the diameter was 35.0 mm. The dry density of the specimen was 1.55 g/cm$^3$.

2.3 Testing procedure

We conducted the wetting process of the water-retention test in which suction was applied by the use of the axis-translation technique (e.g., Lu and Likos 2004). Figure 1 shows a schematic illustration of the procedure of the water-retention test. Beneath the bottom of the specimen, a ceramic disc with an air entry value of 50 kPa was installed in order to sustain the applied suction. The top of the specimen was connected to wet air with atmospheric pressure to prevent the evaporation of water. The degree of humidity of the wet air was no less than 99% and the temperature in the laboratory was kept constant at 20°C throughout the test. On the other hand, the bottom of the specimen was connected to a burette that could be moved vertically. The initial water level of the burette was set to be the same as that at the top of the specimen (Figure 1(a)). Afterwards, a pressure head of minus 100 cm was applied to desaturate the specimen (Figure 1(b)), whose degree of saturation was 13.1%. Then, the prescribed suction potentials were given to the specimen by moving the burette upward (Figure 1(c)), in which the step-by-step increase in the potential of the water in the burette, i.e., a decrease in the suction potential, caused a flow of water from the burette into the specimen. The suction potential is defined as the difference between the top of the specimen and the water level in the burette.

After the increment in water inflow reached almost zero, i.e., the suction potential was equal to the suction inside the specimen, the test apparatus was placed on the work table of the μX-ray CT device and X-ray CT scanning was performed. As shown in Figure 2, we carried out a partial CT scan in which the volume of interest of the specimen is partially scanned with a much higher magnification than that of a normal full CT scan. The scanning area was cylindrical in shape with a height of 3.78 mm and a diameter of 4.35 mm. The scanning location was the middle height of the specimen, 20 mm below the top of the specimen (see Figure 1). The voxel size of the partial CT images was 4.3×4.3×7.0 μm.

## 3. TRINARIZATION OF CT IMAGES FOR PARTIALLY SATURATED SAND

3.1 Histogram of gray values for partially saturated sand

CT images as an assembly of discretized data inherently have ‘mixels’, namely, one voxel containing two or more phases. The gray value for a mixel is obtained as the weighted average value of all the materials in a voxel. This effect is called the partial volume effect (e.g., Curry et al. 1990). The CT images of partially saturated soils contain three types of mixels: the voxels composed of the soil particle phase; the voxels composed of the water phase and the air phase; and the voxels composed of the air phase and the soil particle phase. There are few mixels

composed of all the three phases compared with the other mixels, since they exist only at the points where the three phases face each other, while two phases contact each other over a much wider area of the boundary surfaces.

Figure 3 shows a conceptual illustration of a histogram of CT images for a three-phase coupled partially saturated soil, in which the distributions of the gray values for the three phases are assumed to be similar to the normal distribution. Even a homogeneous single phase usually has a wide variety of gray values as long as X-rays with a broad spectrum are used. We have assumingly drawn the distribution of mixels in a similar shape of normal distribution, since the characterization of the distribution of mixels is known to be difficult. The three phases often overlap each other due to the limitation of spatial resolutions of the current X-ray tomography techniques. Note that the monochromatic X-rays, e.g., generated by synchrotron radiation, may decrease the overlapping.

### 3.2 Region growing method

In order to distinguish the sand particles, the pore water and the pore air from each other, we have trinarized the μX-ray CT images using a region growing method. The region growing method has been developed as one of the region-based segmentation methods for digital images (e.g., Rozenfeld and Kak 1982), which postulates that the neighboring voxels within one region have similar values (e.g., Adams and Bischof 1994). The procedure for the region growing method is schematically illustrated in Figure 4(a). In region growing methods, one voxel, representing one phase, is firstly chosen, which is called ‘seed’. Then, adjacent voxels with similar gray values to the original voxel are assimilated into the same phase. Subsequently, the same procedure is done for the newly assimilated voxels, i.e., the voxels adjacent to the newly assimilated voxels are admitted as the same phase if the gray values are similar to the original one. Repeating these steps eventually leads to one continuous cluster composed of voxels with similar gray values.

The most important features of region growing methods include the assurance of the spatial continuity of the segmented phases, whereas simple thresholds usually only divide the histogram, and the continuity cannot be ensured. Simple thresholds just divide the histogram into three regions. Hence, each region contains more than two phases as well as mixels. In other words, the phases to which the voxels with the same gray values belong cannot be identified with simple thresholds. Some statistical methods have been proposed in which probabilistic distributions of the three phases and the mixels are firstly assumed, and then the histogram is reproduced as a superposition of them. These methods can give the volume of each phase as

well as the mixels, but they cannot provide the spatial positions of the voxels of each phase. On the other hand, region growing methods extract one phase, ensuring continuity and providing spatial positions for all the voxels of the extracted phases as well as the volume of the phases. Watershed techniques (e.g., Vincent and Soille 1991) are also able to provide the spatial positions of segmented voxels, because the images are directly divided into several phases. Since it is important to identify both the spatial positions of the voxels and the volumes of each phase, in order to evaluate the structures of the three phases, a region growing method has been used in the present study.

3.3 Trinarization method for partially saturated sand

Firstly, CT values of each phase were sampled, for which we were able to visually distinguish the three phases since the soil particles, the pore water and the pore air are indicated by light gray, dark gray and black colors, respectively. Secondly, the mean CT value $\bar{x}_i$ $(i = s, w, a)$ and the standard deviation of CT value $\sigma_i$ were calculated for each phase. Usually, ten samples are enough to obtain stable values for $\bar{x}_i$ and $\sigma_i$. In the present study, more than ten samples were taken in all the cases to determine $\bar{x}_i$ and $\sigma_i$. Then, the tolerance values used in the region growing method were determined using $\bar{x}_i$ and $\sigma_i$ based on the normal distribution in which about 95% of values lie within two standard deviation. The tolerance of the air phase was determined as the average value of $\bar{x}_a + 2\sigma_a$ and $\bar{x}_w - 2\sigma_w$, and the tolerance of the soil phase was determined as $\bar{x}_s - 2\sigma_s$ (Figure 4(b)), in which we assumed that the distribution of the CT values for each phase was almost identical to the normal distribution. We employed the average as the tolerance of the air phase, since $\bar{x}_a + 2\sigma_a$ and $\bar{x}_w - 2\sigma_w$ usually overlap each other. Otherwise, we used $\bar{x}_i \pm 2\sigma_i$ directly as in the soil phase.

In the present study, we have employed the normal distributions for all the three phases as a simplest assumption. The log-normal distribution for the air phase is possible option. The distribution obtained in the present study, however, could be similar to normal distribution since X-rays of smaller energy were cut off by copper filter installed just in front of X-ray source.

Using the tolerance values, the region growing method was applied to extract the air phase and the solid phase. The region growing method was performed by the software VGStudio MAX 1.2 (Volume Graphics GmbH) with selectable options of the ‘static’ and ‘dynamic’ region growing. The ‘static’ region growing method was used in this study, in which the gray value of the seed did not change throughout the segmentation. On the other hand, in the ‘dynamic’ region growing, the gray value of the seed is updated every step to the latest average value of all the voxels assimilated. It should be noted that the ‘static’ region growing are not much dependent on seed

point selection compared to the ‘dynamic’ region growing. The region growing method was applied to the soil particle phase and then it was applied to the air phase. The water phase was given as the remaining voxels. For the case in which the pore air was trapped in the pore water, we applied an additional region growing procedure to portions of the air phase.

After the segmentation by the region growing method, the voxels indicating the air phase and the water phase, surrounded only by the soil phase, were converted into the soil phase. This is because the definition of the voids does not include the air or the water in the soil particles. Similarly, the voxels indicating the water phase, surrounded only by the air phase, were converted into the air phase. This is because the pore water is not able to hang in the air. Those converted voxels are probably due to the inherent noise of the μX-ray CT images. Finally, once the trinarization is complete, the proportions of the three phases can be obtained by multiplying the number of voxels for each phase by the unit volume of voxels.

### 3.4 Segmentation of mixels for multi-phase materials

The sub-voxel segmentation of the mixels, i.e., identifying the mixels and quantifying the proportions of the phases in one mixel, is necessary for the exact segmentation of the images. Some evaluation methods for mixels have been reported in previous literature assuming statistical models (e.g., Santago and Gage 1993) and level set techniques (e.g., Rifai et al. 2000).

In the case of multi-phase materials, it is possible that the gray values of the mixels composed of two phases are similar to those of the other phases. As for partially saturated soils, the gray values of the mixels composed of the air phase and the soil particle phase are similar to those of the water phase voxels. This is because the density of the water, 1.0 g/cm$^3$, lies between the densities of the air and the soil particles, almost zero and 2.64 g/cm$^3$, respectively. This makes it more difficult to trinarize the images of multi-phase materials than two-phase materials.

For the above reason, we have not implemented any special treatments to the mixels in this study, e.g., assumption of probabilistic functions for the mixels. The mixels have been segmented by the region growing method based on the proportion of constituents. For example, the mixels with a larger proportion of the soil particle phase than the water phase have probably been assimilated into the soil particle phase. Namely, for partially saturated soils, it is difficult to logically distinguish between the water voxels (absorbed water) and the mixels of soil and air in X-ray CT images.

## 4. RESULTS AND DISCUSSIONS

### 4.1 Water-retention curve

The water-retention curve for the entire specimen during the wetting process is shown in Figure 5. Volumetric water content $\theta$ is defined as the volume of the water divided by the total volume. Thus, the relation between volumetric water content $\theta$ and degree of saturation $S_r$ is $\theta = nS_r$ in which $n$ is the porosity. The water content varies little until a pressure head of around minus 45 cm, step e, is reached. Then, it starts to increase from a pressure head of around minus 40 cm, step f. The rapid increase in water content can be observed at a pressure head of minus 15 cm, from steps k to l, although the change in pressure head is very small. Between these two steps, a pressure head of 5 cm is applied to the specimen, by which the water inflow from the burette to the specimen occurs. The pressure head eventually decreases to almost the same level as that in step k. The volumetric water content finally increases to 0.37 at a pressure head of 0 cm.

### 4.2 Trinarization for high pore saturation region

The locations of the cross sections are indicated in Figure 6. The F-2 vertical cross section includes the center of the specimen; it is parallel and perpendicular to the direction of the X-ray. The A-2 horizontal cross section also includes the center of the specimen. Figure 7 demonstrates the vertical and the horizontal cross sections of the partial CT images and their trinarized images at step l. In this step, a larger amount of pore spaces is occupied by pore water and the pore water seems to be continuous. This kind of high pore saturation region is generally termed “funicular saturation”; the saturation is about 75% in the present study.

In the original CT images, it can be seen that the soil particles indicated by a bright color, the pore water indicated by dark gray and the pore air indicated by black are all distinguished from each other. Note that the white portions indicate iron sand particles naturally included in Toyoura sand. In the trinarized images, the yellow, blue and black portions indicate the soil particles, the pore water and the pore air, respectively. It can be seen that the three phases are obviously distinguished from each other. Pore water exists around the soil particles at the rather small voids, while less pore water is seen at the larger voids.

Using the trinarized images, we have calculated the volume of each phase by multiplying the number of voxels for each phase by the unit volume of the voxels, and have then evaluated the local void ratio and the local degree of saturation of the scan zone. Table 1 shows the proportions of the three phases obtained by the trinarization. The local values are plotted in Figure 5 and indicated by the open l’ mark. The local void ratio is 0.733 and the local degree of

saturation is 73.1%. These local values are comparable to the void ratio and the degree of saturation for the entire specimen, namely, 0.706 and 75.6%, respectively. This suggests that the trinarization method used in this study provides reasonable results for the unsaturated sand in the funicular saturation region.

Since most of the voxels adjacent to the soil particle phase are those of the water phase in the case of the high pore saturation region, the extraction of the soil particle phase by the region growing method is similar to the binarization procedure. This also applies to the extraction of the air phase because almost all the voxels adjacent to the air phase are those of the water phase. Consequently, trinarization in the high pore saturation region rarely encounters problems caused by the boundary between the soil particle phase and the air phase.

4.3 Trinarization in low pore saturation region

We have also applied the same trinarization procedure to the CT images in the low pore saturation region, step k. As can be seen in the original CT images shown in Figure 8, the amount of pore water indicated by light gray is smaller than that of step l and the pore water phase seems to be isolated and discontinuous. This regime is referred to as the “pendular saturation” region.

The trinarized images are shown in Figure 8. The local void ratio of step k is 0.862 which is much larger than that of step l, although the scan zones of the two cases are almost exactly the same. In the low pore saturation region, like the pendular saturation region, there is a wider boundary area between the soil particle phase and the air phase, which tends to make the soil particle voxels and the air voxels into mixels with gray values similar to the water phase due to the partial volume effect. This leads to a reduction in the soil particle voxels, which eventually results in the overestimation of the void ratio. As for the degree of saturation, the local value of step k is 42.0%, similar to that of entire specimen of 45.9%.

We have again applied the region growing method to the soil particle phase with smaller tolerance $T_s$, which provides a larger amount of the soil particle phase, in order to overcome the overestimation of the void ratio. Tolerance $T_s$, was determined to reproduce a similar void ratio to that of step I by trial and error. Then, we have performed the region growing method to extract the air phase from the rest, in which exactly the same tolerance exists for the air phase, $T_a$, as the previous one for step k. The trinarized images are shown in Figure 9 with the original CT image. As shown in Table 1, the proportion of the soil particle phase increases because of the

correction of tolerance $T_s$, while the proportion of the air phase is the same as that without correction because the same tolerance for the air phase, $T_a$, was used. Namely, the proportion of the water phase decreases. This means that the mixels brought about by the partial volume effect of the boundary between the soil particle phase and the air phase are partly converted into the soil particle phase. Consequently, we have obtained a local void ratio of 0.739 that is similar to that for step l.

Some voxels of the water phase, which are not mixels, are also converted into the soil particle phase at the boundary between the soil particle phase and the water phase, by which the number of voxels of the water phase has been underestimated. This is a possible reason why the local degree of saturation, obtained as 36.8%, is smaller than the global degree of saturation of 45.9%. It is worth noting that those water voxels, converted incorrectly, are not many, because the area of the boundary between the soil particle phase and the water phase is basically small in the low pore saturation regime, such as the pendular saturation regime. The other reason is that the vertical distribution of pore water in the specimen was probably caused by the water inflow from the bottom end of the specimen. The pore water is seen to be discontinuous at the scan zone, located at the middle height of the specimen in the original CT images, while the lower part probably contains more water than the scan zone. This suggests that pore water at the lower part and pore water in the scan zone do not fully connect with each other. As seen in the ink-bottle effect (e.g., Lu and Likos), the capillary rise for the wetting process is smaller than that for the drying process since the suction level is determined by the narrower voids located close to the water reservoir. And then, in the next step l, the further decrease in the water potential of 5 cm causes the rapid phase transition from the pendular saturation regime to the funicular saturation regime probably accompanied by the water inflow to a wider area, including the scan zone. Further investigation of the vertical distribution of the pore water is recommended for this point.

## 5. CONCLUSIONS

A trinarization technique, using the region growing method, has been proposed and applied to the μX-ray CT images of partially saturated sand at different water-retention states during the wetting process of the water-retention test. The trinarized images clearly demonstrate the soil phase, the water phase and the air phase. The region growing method ensures the continuity of the extracted phases, the soil particle phase and the air phase in this study, and the spatial positions of the voxels of the three phases.

It has been found that the proposed method can provide reasonable results in the high pore saturation region through a comparison of the void ratio and the degree of saturation between the results obtained by the trinarized images and those measured for the entire specimen. Since the soil particle phase and the air phase mainly make contact with one phase, i.e., the water phase, extracting these phases by the region growing method is similar to binarization.

On the other hand, in the low pore saturation region, there exists a certain amount of boundary between the soil particle phase and the air phase, and the mixels of the boundary among them are likely to have gray values similar to those of the water phase; this results in the overestimation of the void ratio. We would encounter this problem in any segmentation of multi-phase materials, namely, materials having more than two phases. It is impossible, however, to identify the mixels and to quantify the proportions of the phases in one mixel theoretically as long as the CT images are an assembly of the discretized data. It should be noted that we could ignore the effect of the mixels if the spatial resolution of the CT images developed further and became sufficiently high. Unfortunately, due to the limitations of the current techniques, it will still be necessary to implement some sort of validation in order to evaluate the effect of the partial volume effect for segmenting the three phases of partially saturated soils. In the present study, the void ratio has been calibrated against that obtained in the high pore saturation region using a smaller tolerance for soil particle phase $T_s$.

The proposed trinarization technique with validation can visualize the local existence of pore water, by which it is possible to clarify the physical origins of the water-retention behaviour of partially saturated soils, such as the hysteresis of water-retention curves. Note that the proposed method is applicable for uniform sands to find out the microscopic nature of deformation for granular matters. Further studies are necessary for clays and the other materials with finer soil particles and with higher density with use of more advanced visualization and segmentation techniques.

## 6. REFERENCES

Adams, R. and Bischof, L. (1994), Seeded region growing, IEEE Transactions on Pattern Analysis and Machine Intelligence, Vol. 16, No. 6, pp. 641-647.

Bear, J. (1979), Hydraulics of ground water, Dover Publications, Inc., Mineola, NY.

Curry, T.S., Dowdey, J.E. and Murry, R.C. (1990), Christensen's physics of diagnostic radiology,

fourth edition, Lippincott Williams & Wilkins, Philadelphia, PA.

Higo, Y., Oka, F., Kimoto, S., Sanagawa, T. and Matsushima, Y. (2011), Study of strain localization and microstructural changes in partially saturated sand during triaxial tests using microfocus X-ray CT, Soils and Foundations, 51(1), 95-111.

Higo, Y., Oka, F., Sato, T., Matsushima, Y. and Kimoto, S. (2013), Investigation of localized deformation in partially saturated sand under triaxial compression by microfocus X-ray CT with digital image correlation, Soils & Foundations, 53(2), 181-198.

Kohgo, Y., Nakano, M. and Miyazaki, T. (1993), Theoretical aspects of constitutive modelling for unsaturated soils, Soils and Foundations, 33(4), 46-63.

Lu, N. and Likos, W.J. (2004), Unsaturated soil mechanics, John Wiley & Sons, Inc., Hoboken, NJ.

Riedel, I., Andò, E., Salager, S., Bésuelle, P and Viggiani, G. (2012), Water retention behaviour explored by X-ray CT analysis, Unsaturated Soils: Research and Applications, 1, Proceedings of the 2nd European Conference on Unsaturated Soils, 20-22 June 2012, Napoli, Italy, Mancuso, C., Jommi, C. and D'Onza, F., eds., Springer, 81-88.

Rifai, H., Bloch, I., Hutchinson, S., Wiart, I. and Garnero, L. (2000), Segmentation of the skull in MRI volumes using deformable model and taking the partial volume effect into account, Medical Image Analysis, 4, 219-233.

Rosenfeld, A. and Kak, A.C. (1982), Digital picture processing, 2nd edition, Computer Science and Applied Mathematics, Academic Press.

Santago, P. and Gage, H. D. (1993), Quantification of MR brain images by mixture density and partial volume modelling, IEEE Transactions on Medical Imaging, 12(3), 566-574.

Yoshida, T., Higo, Y., Oka, F., Matsushima, Y. (2011), Visualization of microstructures of unsaturated Toyoura sand specimen during water retentivity test, the 24th KKCNN Symposium on Civil Engineering, Hyogo, Japan, December 14-16, 393-396.

Vincent, L. and Soille, P. (1991), Watersheds in digital space, an efficient algorithm based on

immersion simulations, IEEE Transactions on pattern analysis and machine intelligence, Vol. 13, No. 6, pp. 583-598.

Table 1 Proportions of the three phases along with the local void and the local degree of saturation obtained by trinarization

| | Soil particle phase (%) | Air phase (%) | Water phase (%) | Local void ratio | Local degree of saturation (%) |
|---|---|---|---|---|---|
| Step l (High pore saturation region) | 57.7 | 11.4 | 30.9 | 0.733 | 73.1 |
| Step k (Low pore saturation region) | 53.7 | 26.9 | 19.4 | 0.862 | 42.0 |
| Step k with the correction of tolerance $T_s$ (Low pore saturation region) | 57.5 | 26.9 | 15.6 | 0.739 | 36.8 |

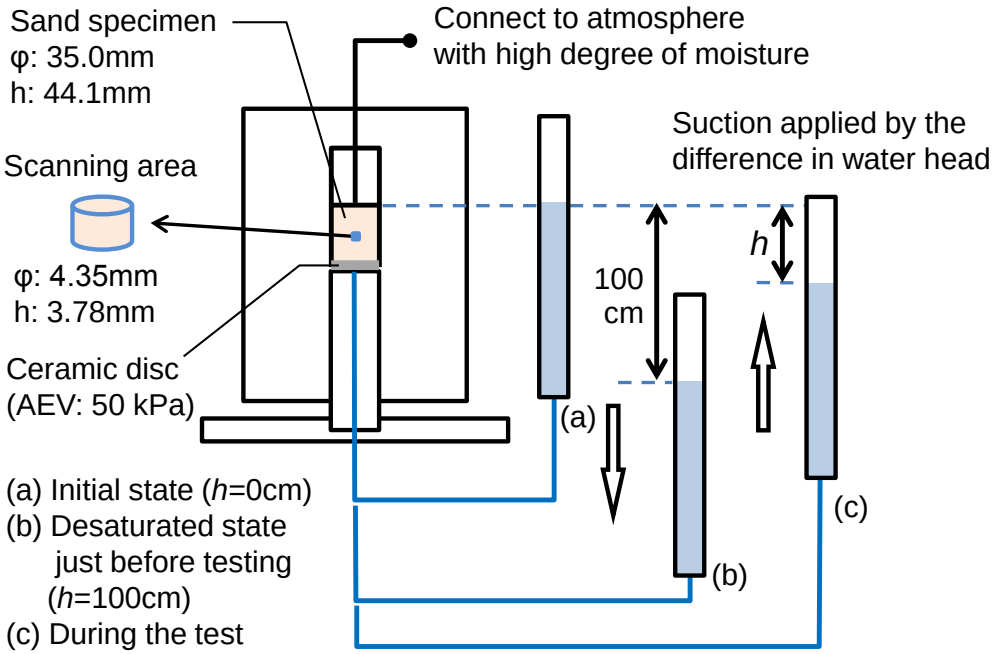


Figure 1 Procedure of the water-retention test

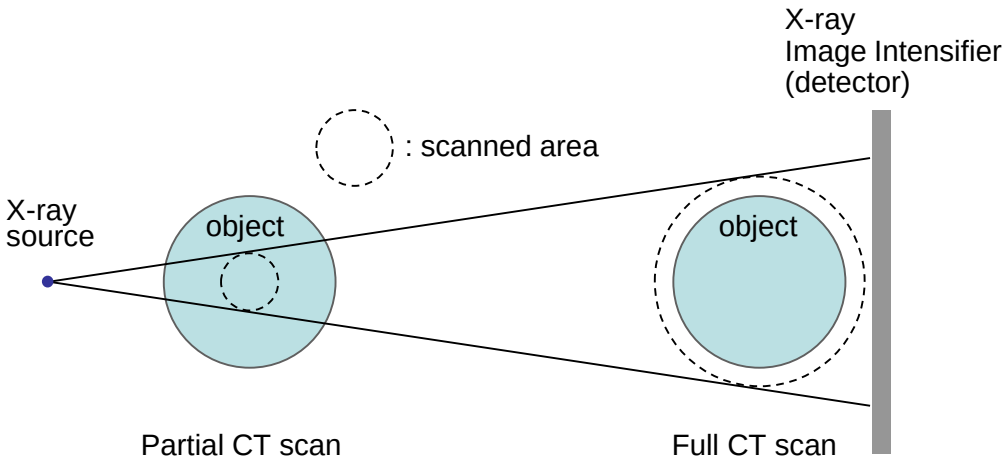


Figure 2 Partial CT scan compared with full CT

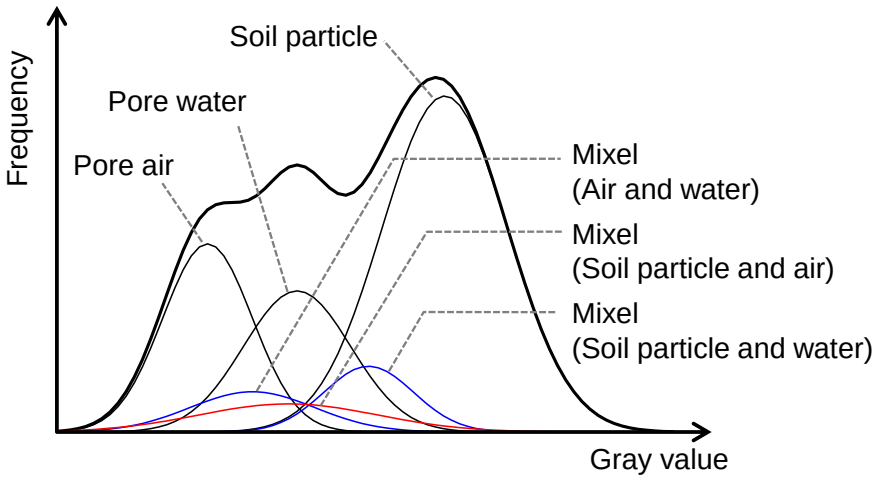


Figure 3 Conceptual illustration of histogram for CT images of partially saturated soil

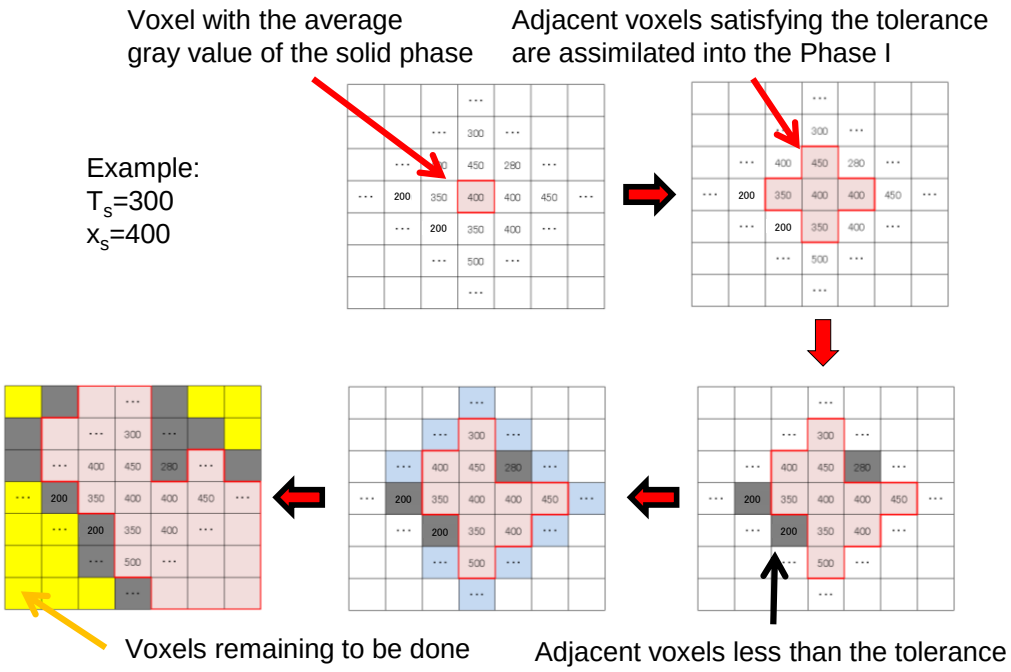


(a)

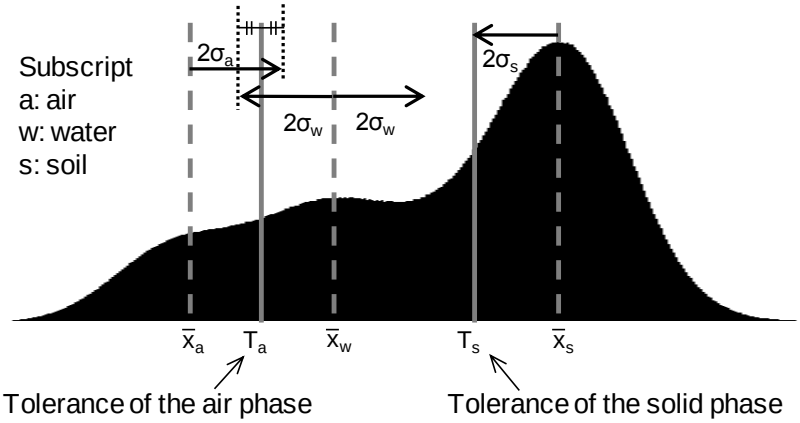


†Note that $T_a$ and $T_s$ are not used for thresholds dividing the histogram but for the tolerances of the region growing method.

(b)

Figure 4 Schematic illustration of region growing method for trinarization technique: (a) procedures and (b) determination of tolerance values

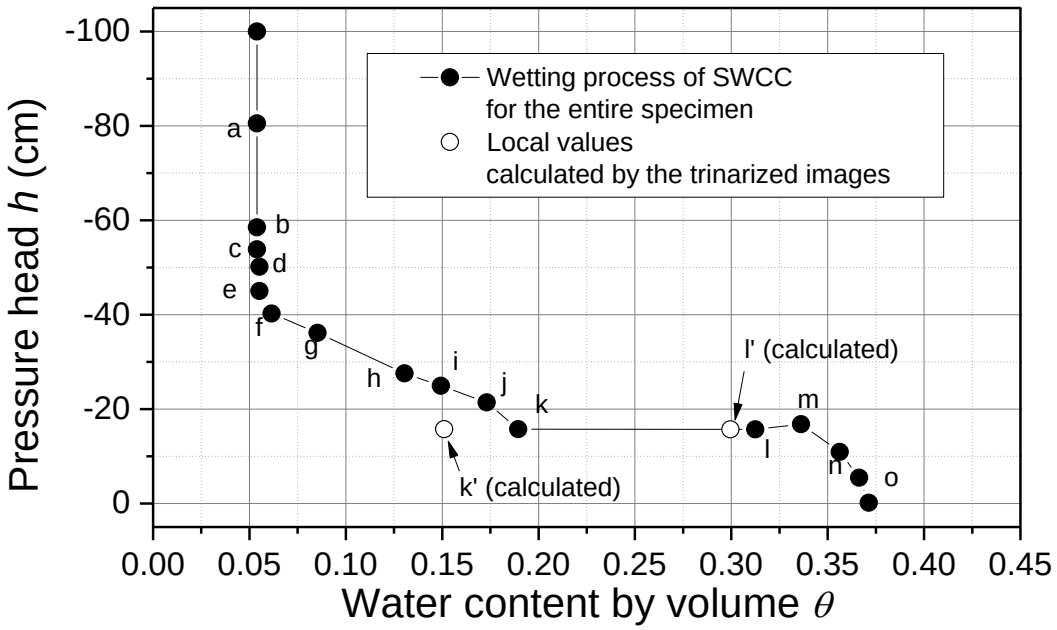


Figure 5 Soil-water characteristic curve and local degree of saturation calculated by trinarized images (X-ray scanning was performed at each step from a to o)

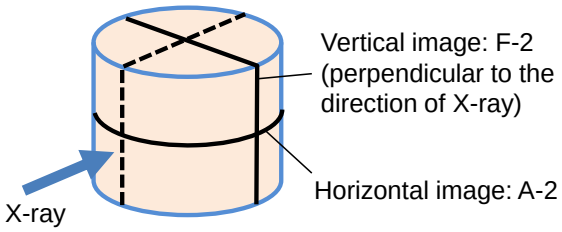


Figure 6 Locations of cross sections

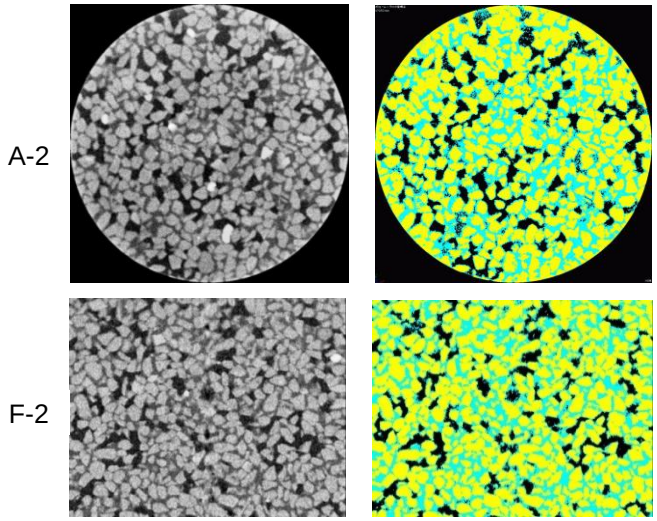


Step l ($S_r$=75.6%, $\theta$=0.31, $h$=-15.7cm)

Figure 7 CT images and their trinarized images in case of high pore saturation regime at step l ($S_r$ and $\theta$ are global values; yellow, blue and black portions indicate the soil particles, the pore water and the pore air, respectively, in the trinarized images)

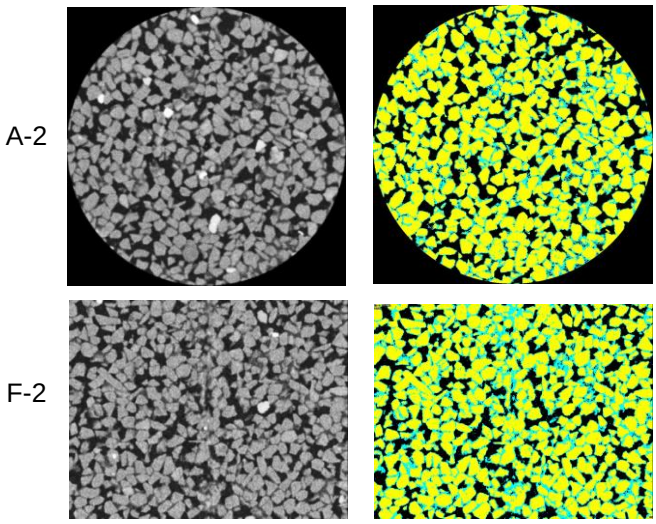


Step k ($S_r$=45.9%, $\theta$=0.19, $h$=-15.8cm)

Figure 8 CT images and their trinarized images in the case of the low pore saturation regime at step k ($S_r$ and $\theta$ are global values; yellow, blue and black portions indicate the soil particles, the pore water and the pore air, respectively, in the trinarized images)

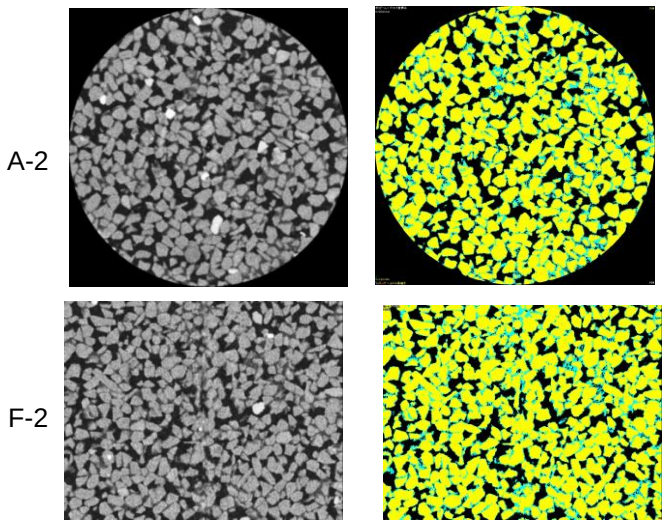


Step k ($S_r$=45.9%, $\theta$=0.19, $h$=-15.8cm)

Figure 9 CT images and their trinarized images with correction of the tolerance in the case of the low pore saturation regime at step k ($S_r$ and $\theta$ are global values; yellow, blue and black portions indicate the soil particles, the pore water and the pore air, respectively, in the trinarized images)